Using of XFEM With Meshing Type-T3 for Orthotropic FGM Plate With A Center Crack Parallel to the Material Gradation Under Fixed Grip Loading

MSc. Hassanein Ibraheem Khalaf & Ass. Prof. Dr. Ameen Ahmed Nassar
Mechanical Engineering Department
College of Engineering University of Basrah
Basrah / Iraq

ABSTRACT

An improved approach for modeling discrete cracks in two-dimensional anisotropic functional graded materials FGMs by XFEM is described. A general node meshing type-T3 with sub-triangle technique for enhancing the Gauss quadrature accuracy near the crack is applied to increase the accuracy of numerical results. Also, the useful incompatible interaction integral method (M-integral method) is used to calculate the stress intensity factors. Numerical simulations have proved that provides accurate results by less number of nodes (DOFs) in comparison with reference. The results of LEFM (liner elastic fracture mechanics) have been compared with the reference results, showing the reliability, stability, and the efficiency of present meshing of XFEM. Matlab program (M-file) is used to solve the aim of this paper.

استخدام طريقه العناصر المحددة المطورة مع شبكة توزيع عقد نوع **T3** لصفيحه تحتوي شرخ متمركز ومتدرجه الخواص المعدنيه وظيفيا وتحت حمل انفعال ثابت

مدرس مساعد حسنين ابراهيم خلف   أستاذ مساعد دكتور امين احمد نصار
قسم الهندسة الميكانيكية
كلية الهندسة
جامعة البصرة
البصرة – العراق

الملخص

البحث يستعرض استخدام منهاج تحسين الطريقه العدديه المطوره XFEM لنمذجه الشروخ في التطبيقات ثنائيه الابعاد وفي معادن متدرجه الخواص وظيفيا. لزيادة دقه الحل، شبكه عقد نوع T3، و تقنية المثلث الفرعية لتوزيع نقاط التكامل العددي عند منطقه الشرخ تم استخدمها. كذلك تم تطبيق طريقه التفاعل التعارضي Incompatible Interaction Integral لحساب معاملات تركيز الاجهاد. اثبت التمثيل العددي الجديد دقته باقل عدد من العقد بالمقارنه مع عدد من المصادر. تم مقارنة نتائج مشاكل الكسر الميكانيكي الخطي

LEFM مع المصادر ذات العلاقه، والتي تبين الاعتمادية، والاستقرار، وكفاءة الطريقه العدديه XEFM مع التقنيات الاخرى المستخدمه.تم استخدام برنامج ماتلاب لحل هدف هذا البحث.

1. INTRODUCTION

Today, functionally graded materials (FGMs) are very significant materials to use in many branches of engineering applications in aerospace, automobile, medical equipments, and turbine industries.

A formulated concept of functionally graded materials (FGMs) was proposed in 1984 by material scientists in Sendai area, Japan, as a means of preparing thermal barrier materials, and a coordinated research was developed in that country since 1986. The idea, that continuously changes in the composition, microstructure, porosity, etc., of these materials resulting in gradients in such properties as mechanical strength and thermal conductivity, has spreaded world-wide in the recent research [1]. Where in these materials smoothly continuously change in microstructure porosity, bonding, etc resulting in gradients in such properties as mechanical strength and thermal conductivity, has spread to use FGMs in different applications rather than use of the ordinary composites by improving a number of useful, relevant properties against the problem of interface regains. Clearly and recently, the use of FGMs rather than composites materials has been developed such as shown in [2-4].

Various method have already presented to the fracture analysis of functionally graded materials. In the calculation of the stress intensity factors in isotropic, the order of singularity of stress field in vicinity of the crack is same as isotropic materials [5]. The study of the fracture analysis of FGMs were increased in the previous forty years. The major information on these types of materials had been extracted by using the numerical methods rather than the theoretical methods that had inability to analyze the complicated material problems. Where, Dolbow and Gosz [6] presented approach that was applicable to the analysis of any FGM in which the form of the asymptotic near-tip fields match those of a homogeneous material and it does not required detailed knowledge of the higher order terms. In the derivation, an interaction energy contour integral was expressed in domain form and evaluated as a post processing step in the X-FEM. Rao and Rahman [7] used meshless method (EFGM) for calculating the fracture parameters of isotropic FGM by developing new two interaction integrals by depending on homogenous and non- homogenous auxiling field. In addition, Kim and Paulino [8] developed with using FEM as a numerical method, an accurate scheme for evaluating mixed-mode SIFs by means of the interaction integral (M-integral) method considering arbitrarily oriented straight and curved cracks in two-dimensional (2D) elastic orthotropic FGMs. The interaction integral proved to be an accurate and robust scheme in the numerical examples where various types of material gradation, such as exponential, radial, and hyperbolic-tangent, were considered. They observed that material orthotropy, material gradation and the direction of material gradation may have a significant influence on SIFs. Dai, et. al. [9] used a meshfree model for the static and dynamic analyses of functionally graded material (FGM) plates based on the radial point interpolation method (PIM). In the method, the mid-plane of an FGM plate was represented by a set of distributed nodes while the material properties in its thickness direction were computed analytically to take into account their continuous variations from one surface to another. Based on the current material gradient, it was found that as the volume fraction exponent increases, the mechanical characteristics of the FGM plate approach those of the pure metal plate blended in the FGM. Also, Kim, and Paulino [10] provided a critical assessment and comparison of three consistent formulations: non-equilibrium, incompatibility, and constant-constitutive-tensor formulations to use in the calculation of stress intensity factor in FGMs. Gao, et. al. [11] presented crack analysis in 2D, with continuously inhomogeneous, isotropic

and linear elastic FGMs. For this purpose, a boundary-domain integral equation formulation was applied. Recently, XFEM fracture analysis of orthotropic functionally graded materials, with orthotropic crack tip enrichments was used by Bayesteh, and Mohammadi [12]. It was cleared that the efficiency of the numerical method in crack analysis of isotropic and anisotropic functionally graded materials (FGMs).

Extended finite element method XFEM [13-14] is a powerful numerical tool in modeling discontinuity and has been taken into consideration in recent years. XFEM is a development of standard finite element method which employs local enrichment of a region using the concept of partition of unity. Consequently, XFEM is moved beyond the limitations of standard finite element method in numerical simulation of discontinuity and also, it has the general advantages of standard FEM. Applying Heaviside function in XFEM, there will be no need to geometric model of crack and as a result, crack propagation problem can be solved without remeshing. Standard FEM employs the ordinary polynomials in modeling cracks and therefore, it is unable to simulate the nonlinear behavior of crack tip and is resulted in mesh dependency of outcomes. Although implementing singular elements is resolved mesh dependency in FEM, the exact displacement field at crack tip can be reproduce by XFEM and there is no mesh.

The type of the element in XEFM is very important for depicting of the behavior of the different complex problems. The division into elements may partly correspond to natural subdivisions of the structure [15].Proved that higher order element such as triangular element gives more fit result in comparing with the analytical solution. Also, the complexity of the material properties   (functionally graded materials FGM, or weak /discontinuous problems) of the whole problem needs proper element with higher order to capture the finest traits of the complex materials [16].

To the best knowledge of authors, XFEM has not been employed to model crack in FGM media under mechanical. So, the purpose of this paper is to study crack in the complex material as FGM mechanical using XFEM with appropriate T3-element. To reach on this goal, formulation of the XFEM model is discussed by considering orthotropic enrichment to achieve higher accuracy and less DOFs. Afterward, changing of the material properties effects on the formulation are represented. Also, the sub-triangular technique for numerical integration near the crack tip, effective nodal distribution near crack tip and for the whole geometry, and interaction integral method (M-integral) with the incompatibility form to calculate SIF are used to capture more accuracy. Numerical example is employed to verify and compare XFEM models with previous reference. All the work is verified by developed code using Matlab environment.

2. FORMULATION OF PROBLEM

In section, governing equations for FGM fracture analysis including stress-strain relationship, stress and displacement field, extended finite element method and standard finite element approach is discussed and the parameters are explained.

2.1 Stress- Strain Relationship

The governing relationship of plane stress-strain in this problem is the form of Hook's low and can be written as [17]

$$\varepsilon^t = \varepsilon^m + \varepsilon^{th} \tag{1}$$

$\varepsilon^t, \varepsilon^m$ and $\varepsilon^{th}$are total, mechanical and thermal strain, respectively. Where ε^m

$$\varepsilon^m_\alpha = \alpha_{\alpha\beta}\sigma_\beta \qquad (\alpha,\beta = 1,2,6) \tag{2}$$

And $\boldsymbol{\varepsilon^{th}}$ equals zero in this work.

In which

$$\varepsilon_1 = \varepsilon_{11}, \quad \varepsilon_2 = \varepsilon_{22}, \quad \varepsilon_6 = 2\varepsilon_{12} \tag{3}$$

$$\sigma_1 = \sigma_{11}, \quad \sigma_2 = \sigma_{22}, \quad \sigma_6 = \sigma_{12} \tag{4}$$

In the case of plane strain, $\alpha_{\alpha\beta}$ should be substituted,

$$\left(a_{ij} - \frac{a_{i3}a_{j3}}{a_{33}}\right) \to a_{ij} \tag{5}$$

As can be seen in Eq. (2), the components of material compliance tensor s_{ijkl} can be expressed by $\alpha_{\alpha\beta}$

$$\begin{bmatrix} a_{11} & a_{12} & a_{16} \\ a_{12} & a_{22} & a_{26} \\ a_{16} & a_{26} & a_{66} \end{bmatrix} = \begin{bmatrix} s_{1111} & s_{1122} & 2s_{1112} \\ s_{2211} & s_{2222} & 2s_{2212} \\ 2s_{1211} & 2s_{1222} & 4s_{1212} \end{bmatrix} \tag{6}$$

Where

$$\varepsilon^m_{ij} = s_{ijkl}\sigma_{kl} \qquad (i,j,k,l = 1,2,3) \tag{7}$$

Considering the stress function $\phi = \phi(x + \mu y)$for an anisotropic case and employing the basic theory of elasticity, the characteristic equation is obtained in the following form

$$a_{11}\mu^4 - 2a_{16}\mu^3 + (2a_{12} + a_{66})\mu^2 - 2a_{26}\mu + a_{22} = 0 \tag{8}$$

It is obvious that the roots of Eq. (8) are complex and can be define in the form of conjugate pairs, $\mu_1, \bar{\mu}_1$ and $\mu_2, \bar{\mu}_2$ [17],

$$\mu_1 = \xi_1 + i\beta_1$$
$$\mu_2 = \xi_2 + i\beta_2 \tag{9}$$

or in the general form of

$$\mu_1 = \mu_2 = \xi + i\beta \tag{10}$$

2.1. Stress and Displacement Field

The displacement and stress field for the problem has been developed [18-19], the obtained asymptotic displacement crack tip can be expressed as

$$u_1 = K_I \sqrt{\frac{2r}{\pi}} Re\left\{\frac{1}{\mu_1-\mu_2}[\mu_1 p_2 g_2(\theta) - \mu_2 p_1 g_1(\theta)]\right\} + K_{II}\sqrt{\frac{2r}{\pi}} Re\left\{\frac{1}{\mu_1-\mu_2}[p_2 g_2(\theta) - p_1 g_1(\theta)]\right\} \tag{11}$$

$$u_2 = K_I \sqrt{\frac{2r}{\pi}} Re\left\{\frac{1}{\mu_1-\mu_2}[\mu_1 q_2 g_2(\theta) - \mu_2 q g_1(\theta)]\right\} + K_{II}\sqrt{\frac{2r}{\pi}} Re\left\{\frac{1}{\mu_1-\mu_2}[q_2 g_2(\theta) - q_1 g_1(\theta)]\right\} \tag{12}$$

where (X, Y) are considered the components of global coordinate system, (x, y) the components of the local crack tip system and the local crack tip polar coordinate system (r, θ) can be defined by $x+iy=re^{i\theta}$, which are demonstrated in **Figure (1).** Moreover, Re implies the real part of complex displacement functions. Also, u_1 and u_2 are defined as the components of displacement in x and y directions, respectively.

$$g_i(\theta) = \sqrt{cos(\theta) + \mu_i \, sin(\theta)} \qquad (i = 1,2) \tag{13}$$

$$p_k = a_{11}\mu_k^2 + a_{12} - a_{16}\mu_k \qquad (k = 1,2) \tag{14}$$

$$q_k = a_{12}\mu_k + \frac{a_{22}}{\mu_k} - a_{26} \qquad (k = 1,2) \tag{15}$$

Furthermore, the components of asymptotic stress are in the form of

$$\sigma_{11} = \frac{K_I}{\sqrt{2\pi r}} Re\left\{\frac{\mu_1\mu_2}{\mu_1-\mu_2}\left[\frac{\mu_2}{g_2(\theta)} - \frac{\mu_1}{g_1(\theta)}\right]\right\} + \frac{K_{II}}{\sqrt{2\pi r}} Re\left\{\frac{1}{\mu_1-\mu_2}\left[\frac{\mu_2^2}{g_2(\theta)} - \frac{\mu_1^2}{g_1(\theta)}\right]\right\} \tag{16}$$

$$\sigma_{22} = \frac{K_I}{\sqrt{2\pi r}} Re\left\{\frac{1}{\mu_1-\mu_2}\left[\frac{\mu_1}{g_2(\theta)} - \frac{\mu_2}{g_1(\theta)}\right]\right\} + \frac{K_{II}}{\sqrt{2\pi r}} Re\left\{\frac{1}{\mu_1-\mu_2}\left[\frac{1}{g_2(\theta)} - \frac{1}{g_1(\theta)}\right]\right\} \tag{17}$$

$$\sigma_{12} = \frac{K_I}{\sqrt{2\pi r}} Re\left\{\frac{\mu_1\mu_2}{\mu_1-\mu_2}\left[\frac{1}{g_1(\theta)} - \frac{1}{g_2(\theta)}\right]\right\} + \frac{K_{II}}{\sqrt{2\pi r}} Re\left\{\frac{1}{\mu_1-\mu_2}\left[\frac{\mu_1}{g_1(\theta)} - \frac{\mu_2}{g_2(\theta)}\right]\right\} \tag{18}$$

In the FGMs, the components of material compliance tensor, a_{ij}, are changing on the material volume. As a result, there are different amount of p_k, q_k, and μ_k at one point compared to another.

For this reason, material properties for the auxiliary field (in contour integral) and crack tip enrichment functions are calculated at the crack tip.

According to the explanations, the parameter χ_k should be replaced with χ_k^{tip} in Eqs. (11-18) to modify the equations for the FGM materials.

$$\chi_k \rightarrow \chi_k^{tip} \tag{19}$$

where χ_k is the representation of a_{ij}, p_k, q_k and μ_k , and χ_k^{tip} states these parameters at the crack tip.

2. STRESS INTENSITY FACTORS

2.1. Calculating J-Integral

Non-equilibrium, incompatibility, and constant-constitutive-tensor are three different methods have been employed by Kim et al [10] for this side. The incompatibility formulation is employed in this paper as the method is used to approximate J-integral for the reseason that this procedure requires less complicated derivatives with the same accuracy of non- equilibrium formulation [10,19]. Also, constant-constitutive-tensor method leads to inaccuracy with C^0 finite element formulation. The incompatibility procedure satisfies the following equations

$$\sigma_{ij} = c_{ijkl}(x)\varepsilon_{kl}^m \ , \ \ \varepsilon_{ij} \neq \frac{1}{2}\big(u_{i,j} + u_{j,i}\big), \ \ \sigma_{ij,j} = 0 \tag{20}$$

which includes constitutive and equilibrium equations and $\boldsymbol{c_{ijkl}}$ is the material modulus while it does not satisfy compatibility.

Inversing the first part of Eqs. (20) yields

$$\varepsilon_{kl}^m = s_{ijkl}(x)\sigma_{kl} \tag{21}$$

where $s=c^{-1}$. On the whole, Using the equivalent domain integral **(Figure (2))**, J-integral can be expressed as

$$J = \int_A \big(\sigma_{ij}u_{i,1} - w\delta_{1j}\big)q_{,j}dA + \int_A \big(\sigma_{ij}u_{i,1} - w\delta_{1j}\big)_{,j}qdA \tag{22}$$

where q is a smooth function from $q=1$ on interior boundary of A and $q=0$ on the outer one, as depicted in **Figure (2)**. And n_j is the jth component of the outward unit normal to Γ, δ_{ij} is the Kronecker delta and the Cartesian coordinate system whose x axis is parallel to the crack surface. w is the strain energy density which can be presented as

$$w = \frac{1}{2}\big(\sigma_{11}\varepsilon_{11}^m + \sigma_{22}\varepsilon_{22}^m + 2\sigma_{12}\varepsilon_{12}^m\big) \tag{23}$$

For plane stress and

$$w = \frac{1}{2}(\sigma_{11}\varepsilon_{11}^m + \sigma_{22}\varepsilon_{22}^m + \sigma_{33}\varepsilon_{33}^m + 2\sigma_{12}\varepsilon_{12}^m) \tag{24}$$

For plane strain. Since in the plane strain condition,

$$\varepsilon_{33}^t = 0 \ \rightarrow \varepsilon_{33}^m = -\varepsilon_{33}^{th} = -\alpha_{33}\Delta T \tag{25}$$

Eq. 25 is useful if the analyze is done with thermal and mechanical load.

2.2 Different Parts of Stress Intensity Factors

To calculate stress intensity factors of mode I and II, the interaction integral is applied. J^s can be divided into three components including J, J^{aux} and M^l

$$J^s = J + J^{aux} + M^l \tag{26}$$

In which the auxiliary and actual field J-integral are expressed by J^{aux} and J , respectively. Considering

$$\sigma_{ij}^{aux}u_{i,1j} = \frac{1}{2}\sigma_{ij}^{aux}\left(u_{i,1j} + u_{j,1i}\right) = \sigma_{ij}^{aux}\varepsilon_{ij,1}^t = \sigma_{ij}^{aux}(\varepsilon_{ij,1}^m + \varepsilon_{ij,1}^{th}) \tag{27}$$

interaction integral M^l can be expressed as

$$M^l = M^m + M^{th} \tag{28}$$

where by some manipulating, M^m can be expressed as

$$M^m = \int_A \left\{\sigma_{ij}u_{i,1}^{aux} + \sigma_{ij}^{aux}u_{i,1} - \frac{1}{2}(\sigma_{ik}\varepsilon_{ik}^{aux} + \sigma_{ik}^{aux}\varepsilon_{ik}^m)\delta_{1j}\right\}q_{,j}dA$$

$$+ \int_A \left\{\sigma_{ij}\left(s_{ijkl}^{tip} - s_{ijkl}(x)\right)\sigma_{kl,1}^{aux}\right\}qdA \tag{29}$$

It should be mentioned that there is no thermal effect in auxiliary field and ε^{aux} is mechanical strain. Also,

$$\sigma_{33}\varepsilon_{33}^{aux} = \sigma_{33}^{aux}\varepsilon_{33}^{m} = 0 \tag{30}$$

In the plane stress condition. Furthermore

$$\sigma_{33}\varepsilon_{33}^{aux} = 0 \quad \text{and} \quad \sigma_{33}^{aux}\varepsilon_{33}^{m} \neq 0 \tag{31}$$

In an elastic media, the released energy rate can be expressed as

$$G = J = c_{11}K_I^2 + c_{12}K_IK_{II} + c_{22}2K_{II}^2 \tag{32}$$

Where

$$c_{11} = -\frac{a_{22}}{2}Im\left(\frac{\mu_1+\mu_2}{\mu_1\mu_2}\right) \tag{33}$$

$$c_{12} = -\frac{a_{22}}{2}Im\left(\frac{1}{\mu_1\mu_2}\right) + \frac{a_{11}}{2}Im(\mu_1\mu_2) \tag{34}$$

$$c_{22} = \frac{a_{11}}{2}Im(\mu_1 + \mu_2) \tag{35}$$

The effect of two superimposed fields can be considered using the expression [20]

$$M^l = 2c_{11}K_I^{aux}K_I + c_{12}(K_I^{aux}K_{II} + K_{II}^{aux}K_I) + 2c_{22}K_{II}^{aux}K_{II} \tag{36}$$

Substituting $K_I^{aux} = 1, K_{II}^{aux} = 0$ and $K_I^{aux} = 0, K_{II}^{aux} = 1$ into Eq. (36), the equation will be simplified in the form of

$$\begin{cases} M_1^l = 2c_{11}K_I + c_{12}K_{II} & (K_I^{aux} = 1 \text{ and } K_{II}^{aux} = 0) \\ M_2^l = c_{12}K_I + 2c_{22}K_{II} & (K_I^{aux} = 0 \text{ and } K_{II}^{aux} = 1) \end{cases} \tag{37}$$

and stress intensity factors of actual modes I and II can be achieved easily.

2.3 A Review of Extended Finite Element Method

The extended finite element method (XFEM) is a numerical method has been implemented comprehensively for fracture analysis of various problems in past two decades. XFEM is a standard

finite element method development which is more appropriate for the problems with discontinuity and singular fields. The partition of unity finite element method PUFEM can be implemented to create more convergent and effective numerical methods. XFEM employed the concept of partition of unity (PU) to reproduce the displacement, strain and stress fields. The minimum requirement for a function g_k which can be used in PU is to satisfy the following condition [13]

$$\sum_{k=1}^{m} g_k(x) = 1 \quad (x \in \Omega_{PU}) \tag{38}$$

The definition of reproducing condition or completeness can be considered for an arbitrary function ψ in the domain of Eq. (38) and yields,

$$\sum_{k=1}^{m} g_k(x)\psi(x) = \psi(x) \quad (x \in \Omega_{PU}) \tag{39}$$

As the set of isoparametric finite element shape functions N_i , satisfy Eq. (38), these functions can be employed as local enrichment functions to reproduce the desired fields

$$\phi^{enr} = \sum_{i \in N_{enr}} N_i(x)\psi(x)a_i \quad (x \in \Omega_{enr}) \tag{40}$$

where N_{enr} expresses the enriched nodes, N_i are the shape functions and a_i are the additional DOFs. Considering M collection as the following

$$M = \{\psi_1, \psi_2, \dots, \psi_m\} \tag{41}$$

The arrays of M are the enrichment functions. Introducing Eq. (41) into Eq. (40) gives

$$\phi^{enr} = \sum_{i \in N_{enr}} N_i(x)\left(\sum_{m \in M} \psi_m(x)a_{im}\right) \quad (x \in \Omega_{enr}) \tag{42}$$

To accurate the results of the solution, small elements with higher order (T3-triangular elements) are used rather than Q4 (quadratic elements) elements of the relevant references. The T3-elements are used for whole domain to control on behaviors of the complex materials such as FGMs.

Employing XFEM, the obtained displacement field will be added to the displacement field achieved by standard finite element method in the form of

$$\boldsymbol{u} = \boldsymbol{u}^{FEM} + \boldsymbol{u}^{XFEM} \tag{43}$$

In which $\boldsymbol{u}^{XFEM}$ can be expressed (for the element near the crack) as

$$\boldsymbol{u}^{XFEM} = \boldsymbol{u}^{Tip} + \boldsymbol{u}^{He} + \boldsymbol{u}^{Blend} \tag{44}$$

where $\boldsymbol{u}^{Tip}$, $\boldsymbol{u}^{He}$ and $\boldsymbol{u}^{Blend}$ are the displacement of tip enrichment domain, Heaviside enrichment domain and transition domain, respectively.

On the whole, discretization of domain geometry in XFEM is performed in the same way of the traditional finite element method.

$$\boldsymbol{x} = \sum_{i\in\Omega} N_i(\xi,\eta)\, \hat{\boldsymbol{x}}_i \tag{45}$$

To describe and to model the crack, level set method is used [13]. In this approach, only nodal data were used to describe the crack; no geometrical entity was introduced for the crack trajectory, and no partial differential equations need to be solved to update the level sets as that needed in conventional FEM. Where, the nodal description can be updated as the shape function equations.

3. ENRICHMENTS

3.1 Heaviside Enrichment for Discontinuity

The XFEM ability in simulating discontinuity is originated from applying Heaviside function for enrichment. Different types of Heaviside function are proposed in the literature, one of these form is

$$H(\xi) = \begin{cases} 1 & \forall \xi > 0 \\ -1 & \forall \xi < 0 \end{cases} \tag{46}$$

In which to evaluate the amount of $\xi(\boldsymbol{x})$, the sign distance function is implemented, as shown in **Figure (3)**.

For a point $\boldsymbol{x}$ in the Heaviside enriched domain, and $\boldsymbol{x}_\Gamma$ as the projection of point $\boldsymbol{x}$ on the crack, $\xi(\boldsymbol{x})$ is defined as

$$\xi(\boldsymbol{x}) = \boldsymbol{d}.\boldsymbol{n}_x^\Gamma \tag{47}$$

In which

$$\boldsymbol{d} = \boldsymbol{x} - \boldsymbol{x}_\Gamma \tag{48}$$

and the unit normal vector of crack line at $\boldsymbol{x}_\Gamma$ is denoted by $\boldsymbol{n}_x^\Gamma$.

Considering S as the set of nodes which have the Heaviside function enrichment, $\boldsymbol{u}^{He}$ can be expressed as

$$\boldsymbol{u}^{He} = \sum_{i\in S} N_i(\boldsymbol{x})H(\xi)\,\hat{\boldsymbol{a}}_i \tag{49}$$

3.2 Enrichments at the Crack Tip

He implementing of enrichment functions at the crack tip leads to reproducing the highly non-linear stress and displacement fields around the crack with higher accuracy. Due to the difference between the behavior of these fields near the crack and other areas, the standard finite element shape functions are not able to approximate the fields in both areas with high accuracy. Consequently, considering appropriate crack tip enrichments in the elements near the crack tip can improve the obtained results in this area. The enrichments will be determined according to the nature of these fields. Considering F as a set of tip enrichments, yields,

$$F = \{f_1, f_2, \dots, f_m\} \tag{50}$$

The displacement field at the crack field can be estimated by

$$\boldsymbol{u}^{Tip} = \sum_{i\in Tip} N_i(\boldsymbol{x})\left(\sum_{k\in F} f_k(\boldsymbol{x})\hat{\boldsymbol{b}}_{ik}\right) \tag{51}$$

Where *Tip* are the enriched nodes using the tip enrichments functions and $\hat{\boldsymbol{b}}_{ik}$ are the extra DOFs due to the enrichments. The chosen tip enrichments functions for isotropic homogeneous materials can be represented in the form of [21-22].

$$F = \left\{\sqrt{r}\,\sin\left(\tfrac{\theta}{2}\right), \sqrt{r}\,\cos\left(\tfrac{\theta}{2}\right), \sqrt{r}\,\sin\left(\tfrac{\theta}{2}\right)\sin(\theta), \sqrt{r}\,\cos\left(\tfrac{\theta}{2}\right)\sin(\theta)\right\} \tag{52}$$

3.3 Obtaining Displacement Field in XFEM

Introducing Heaviside and tip enrichment displacement field in standard finite element method displacement field gives [21-22].

$$\boldsymbol{u}(\boldsymbol{x}) = \left[\sum_{i\in I} N_i(\boldsymbol{x})\hat{\boldsymbol{u}}_i\right] + \left[\sum_{s\in S} N_s(\boldsymbol{x})\big(H(\xi)\big)\hat{\boldsymbol{a}}_s\right] + \left[\sum_{t\in Tip} N_t(\boldsymbol{x})\left(\sum_{k\in F} f_k(\boldsymbol{x})\hat{\boldsymbol{b}}_{kt}\right)\right] \tag{53}$$

where the first expression is corresponding to standard finite element method, Heaviside enrichment and tip enrichment.

3.4 Enrichment Functions for Orthotropic Materials

Increasing number of studies on orthotropic materials, more researches are performed in obtaining enrichment functions for these materials. Several functions for crack tip enrichment are achieved by the following expression is proposed in the polar local coordinate for crack tip enrichment [21-23].

$$F(r,\theta) = \left\{ \sqrt{r}\,\cos\left(\tfrac{\theta_1}{2}\right)\sqrt{g_1(\theta)}, \sqrt{r}\,\cos\left(\tfrac{\theta_2}{2}\right)\sqrt{g_2(\theta)}, \sqrt{r}\,\sin\left(\tfrac{\theta_1}{2}\right)\sqrt{g_1(\theta)}, \sqrt{r}\,\sin\left(\tfrac{\theta_2}{2}\right)\sqrt{g_2(\theta)} \right\} \quad (54)$$

Where

$$g_j(\theta) = \sqrt{\left(\cos(\theta) + \xi_j\,\sin(\theta)\right)^2 + \left(\beta_j\,\sin(\theta)\right)^2} \quad (j = 1,2) \tag{55}$$

$$\theta_k(\theta) = \tan^{-1}\left(\frac{\beta_k\,\sin(\theta)}{\cos(\theta) + \xi_k\sin(\theta)}\right) \quad (k = 1,2) \tag{56}$$

In which ξ_i and β_i are the same as Eq. (10).

4. NUMERICAL INTEGRATION

Usually the Gauss quadrature rule is employed for numerical integration inside the background cell. Generally, four Gauss points are used in the standard four-node cell. Existence of discontinuity within a background cell may result in substantial accuracy reduction. Also, many researchers demonstrated that a regular increase in order of Gauss integration does not necessarily improve the integration over a discontinuous element/cell, whereas independent integration of each side of the discontinuity with even low order rules does guarantee an accurate integration [19]. So, an efficient technique is required to define the necessary points needed for the integration within these background cells, while remains consistent with the crack geometry. An approach similar to the one proposed by [24] and originally utilized by [19] is adopted for the first time for fracture analysis of FGMs by EFGM. Any background cell which intersects with a crack is subdivided at both sides into sub-triangles whose edges are adapted to the crack faces, as illustrated in **Figure (2)**. It is important to note that, while triangulation of the crack tip element substantially improves the accuracy of integration by increasing the order of Gauss quadrature, it also avoids numerical complications of singular fields at the crack tip because none of the Gauss points are placed on the position of the crack tip.

5. NUMERICAL CASE STUDY

Proper case study is presented in this section to illustrate the application of the XEFM with T3-element for crack analysis of functionally graded materials (FGMs). To accurate the results of the solution, small elements with higher order (T3-triangular elements) are used for the whole problem. The T3-elements are used for whole domain to control on behaviors of the complex material properties such as in the behavior of FGMs. Matlab program (M-file) is used to illustrate the aim of this paper.

The sub-triangular technique near the crack tip (13 gauss point at crack tip and with crack surface, and 7 gauss points for others), the proper nodal distribution for local crack region and for the whole geometry, and the interaction integral method with the incompatibility formulation to calculate SIFs are used the crack analysis in FGM. The level set method is used to represent the crack.

Therefore, A square plate with a center crack is presented (L/W=1), as shown in Fig. 5. A center crack of length 2a located in a finite two-dimensional plate under fixed grip loading, the complete finite element mesh, a mesh detail with mesh type T3, and a zoom of the crack tip region, are depicted **in**

Figure (6) and (7) respectively. For fixed-grip loading, the applied load results in uniform strain $\varepsilon_{22}(X_1, X_2) = \varepsilon_0$ for a corresponding uncracked plate.

The variations of E_{11}, E_{22}, and G_{12} are assumed to be an exponential function of x_1 and proportional to one another, while the Poisson's ratio v_{12} is constant ($v_{12} = 0.3$ and $k_0 = 0.5$). The XFEM mesh has 3042 T3, with 1600 nodes as shown in **Figure (6)** for mesh distribution, where the nodes are applied on the edges of elements to be following the rules of background technique that explain well in [17, 20]. Comparison well be made with [25] that used mesh 1666 Q8, 303 T6, and 32T6qp crack-tip singular finite elements with a total of 2001 elements and 5851 nodes. Firstly, the present work will be less time cost where DOFs less than that used in reference [25].

The following data were used for the XFEM analysis:

$$E_{11} = E_{11}^0 \, e^{\beta X_1}, \; E_{22} = E_{22}^0 \, e^{\beta X_1}, \; G_{11} = G_{11}^0 \, e^{\beta X_1}, \frac{a}{W} = 0.1, \; L/W = 1$$

$$\beta a = 0 - 1, E_{11}^0 = 10000 \, N/mm^2, E_{22}^0 = 1000 N/mm^2, G_{12}^0 = 1216 \, N/mm^2$$

It can be observed from **Table (1)** that the good agreement of the normalized SIF of the present work in comparison with the reference value under the changing of material non-homogeneity of functionally graded material. Where six statues of the material properties changing is taken as explain in **Table (1).**

To further verification of present work on the solution accuracy and the stability of T3-element using with other useful applied techniques, **Figure (8)** clearly shows that no sensitivity (very small change) is occurred at the change of the radius of J integral/a (0.2-1) with the value of the normalized stress intensity factor. So, from **Table (1)** and **Figure (8)**, one can show the stability and good agreement of the present work with less DOFs in comparing with the relevant reference. Incompatible M-integral method is used to calculate the stress intensity factors as explain in section 2.

The problem that studied and presented is done by developing a MATLAB code. All items of the XFEM and the applied-fracture mechanics LEFM are presented completely. So in the programming package, any geometry preprocessing and post-processing with any boundary conditions and substations, and other advanced problems can be easily depicted and studied.

6. CONCLUSION

The development of this work for isotropic and FGMs crack analysis by XEFM that uses of the T3-element, sub-triangle technique for the numerical integration, with proper enrichment functions in the crack location has significantly increased the accuracy of the solution. The triangulation (element and technique) substantially improves the accuracy of integration by increasing the order of DOFs/ Gauss quadrature. The use of the interaction integral method with the mode of the incompatibility provides very accurate answers for the values of SIFs. The study of thermal loading on crack in FGMs is required for the future work.

REFERENCES

[1] Shiota, and Y. Miyamoto "Functionally graded materials 1996" Elsevier Science, Proceedings of the 4th international symposium on Functionally Graded Materials, AIST Tsukuba Research center, Tsukuba, Japan, October 21-24,1996.

[2] Huaiwei Huang, and Qiang Han, "Stability of pressure-loaded functionally graded cylindrical shells with inelastic material properties ",Thin-Walled Structures, Volume 92, July 2015, Pages 21-28.

[3] H. Salehipour, A.R. Shahidi, andf H. Nahvi, "Modified nonlocal elasticity theory for functionally graded materials", International Journal of Engineering Science, Volume 90, May 2015, Pages 44-57.

[4] Ugurcan Eroglu, "In-plane free vibrations of circular beams made of functionally graded material in thermal environment: Beam theory approach", Composite Structures, Volume 122, April 2015, Pages 217-228.

[5] F. Delale and F. Erdogan, "The crack problem for a non-homogeneous plate" , ASME Journal of Applied Mechanics, 50(3), 609–614, 1983.

[6] J.E. Dolbow , and M. Gosz, "On the computation of mixed-mode stress intensity factors in functionally graded materials" International Journal of Solids and Structures 39 (2002) 2557–2574.

[7] B.N. Rao, and S. Rahman, "Mesh-free analysis of cracks in isotropic functionally graded materials" Engineering Fracture Mechanics 70 (2003) 1–27.

[8] J.-H. Kim, and G. H. Paulino, "An accurate scheme for mixed-mode fracture analysis of functionally graded materials using the interaction integral and micromechanics models" Int. J. Numer. Meth. Engng 2003; 58:1457–1497.

[9] K. Y. Dai, G. R. Liu, K. M. Lim, X. Han, and S. Y. Du, "A meshfree radial point interpolation method for analysis of functionally graded material (FGM) plates" Computational Mechanics 34 (2004) 213–223 ,Springer-Verlag 2004.

[10] J.-H. Kim, and G. H. Paulino, "Consistent Formulations of the Interaction Integral Method for Fracture of Functionally Graded Materials" Journal of Applied Mechanics ,ASME- May 2005, Vol. 72, pp 351-364.

[11] A. Asadpoure, S. Mohammadi, and A. Vafaia, "Modeling crack in orthotropic media using a coupled finite element and partition of unity methods" Finite Elements in Analysis and Design 42 (2006) 1165 – 1175.

[12] Alireza Asadpoure, Soheil Mohammadi, and Abolhasan Vafai, "Crack analysis in orthotropic media using the extended finite element method" Thin-Walled Structures 44 (2006) 1031–1038

[13] T. Belytschko and T. Black, "Elastic crack growth in finite elements with minimal remeshing", International Journal for Numerical Methods in Engineering 45 (5): 601-620 (1999).

[14] Zhuo Zhuang, Zhanli Liu, Binbin Cheng and Jianhui Liao , " Extended Finite Element method ", Tsinghua University Press Computational Mechanics Series, 2014 Elsevier Inc.

[15] H. Grandin Jr., Fundamentals of the Finite Element Method, , Macmillan, New York 1986.

[16] Q.-Z. Zhu. "On enrichment functions in the extended finite element method", International Journal for Numerical Methods in Engineering, Wiley-Blackwell, 2012, 91 (2), pp.186-217.

[17] Lekhnitskii, S.G., "Theory of an anisotropic elastic body", MIR -PUBLISHER, MOSCW, 1981.

[18] Sih, G.C., Paris, P.C., Irwin, G.R., On cracks in rectilinearly anisotropic bodies. International Journal of Fracture Mechanics, 1965: p. 189-203.

[19] S.S. Hosseini, H. Bayesteh, S. Mohammadi, "Thermo-mechanical XFEM crack propagation analysis of functionally graded materials", Materials Science & Engineering A 561 (2013) 285–302

[20] Wang, S.S., Yau, J.F., Corten, H.T. , "A mixed mode crack analysis of rectilinear anisotropic solids using conservation laws of elasticity". International Journal of Fracture, 1980. 16: p. 247-259.

[21] Soheil Mohammadi, " EXTENDED FINITE ELEMENT METHOD for Fracture Analysis of Structures " First published 2008 by Blackwell Publishing Ltd.

[22] Soheil Mohammadi, " XFEM FRACTURE ANALYSIS OF COMPOSITES" First published 2012 by 2012 John Wiley & Sons, Ltd.

[23] A. Asadpoure, and S. Mohammadi, "Developing new enrichment functions for crack simulation in orthotropic media by the extended finite element method" Int. J. Numer. Meth. Engng 2007; 69:2150–2172

[24] J. Dolbow "An extended finite element method with discontinuous enrichment for applied mechanics", Theor Appl Mech, Ph.D. thesis. Northwestern University, Evanston, IL, USA, 1999.

[25] J.-H. Kim, and G. H. Paulino, "The interaction integral for fracture of orthotropic functionally graded materials: evaluation of stress intensity factors" International Journal of Solids and Structures 40 (2003) 3967–4001.

Table (1): The effecting of material non-homogeneity on normalized mode I SIF in a non-homogeneous orthotropic plate under fixed grip loading

βa	$K_I(-a)/K_0$ (present)	$K_I(-a)/K_0$ [25] M integral	$K_I(-a)/K_0$ [25] MCC
0.00	0.9958	0.9969	0.9986
0.10	0.9267	0.9247	0.9251
0.25	0.8307	0.8245	0.8233
0.50	0.6717	0.6706	0.6680
0.75	0.5341	0.5404	0.5358
1.00	0.4250	0.4335	0.4285
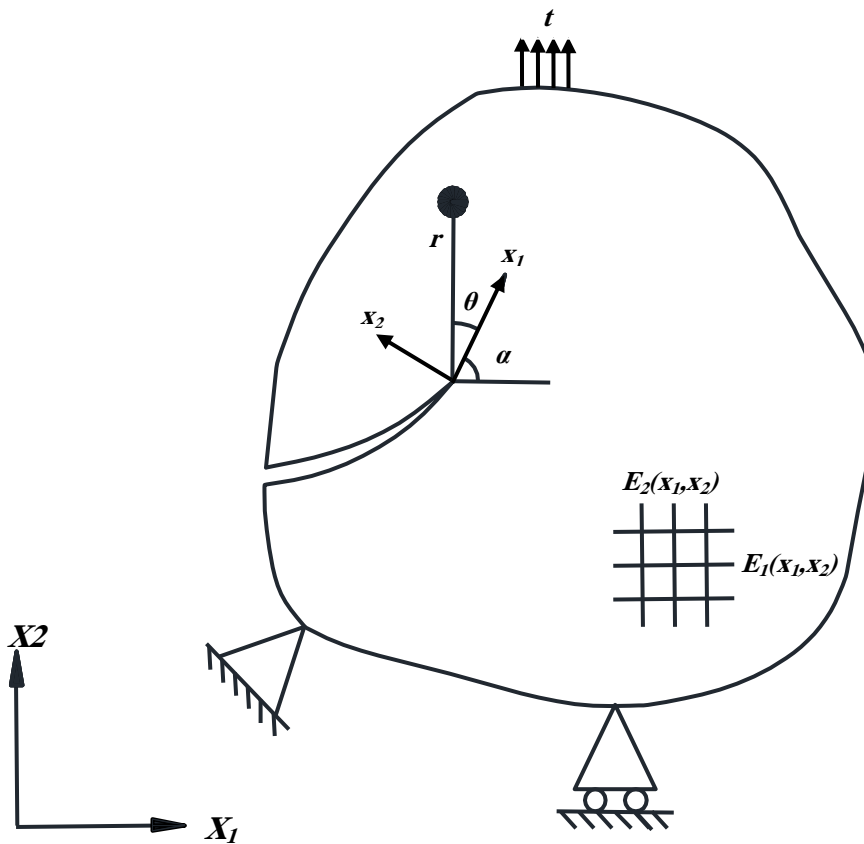
Figure (1): Crack Tip Geometry
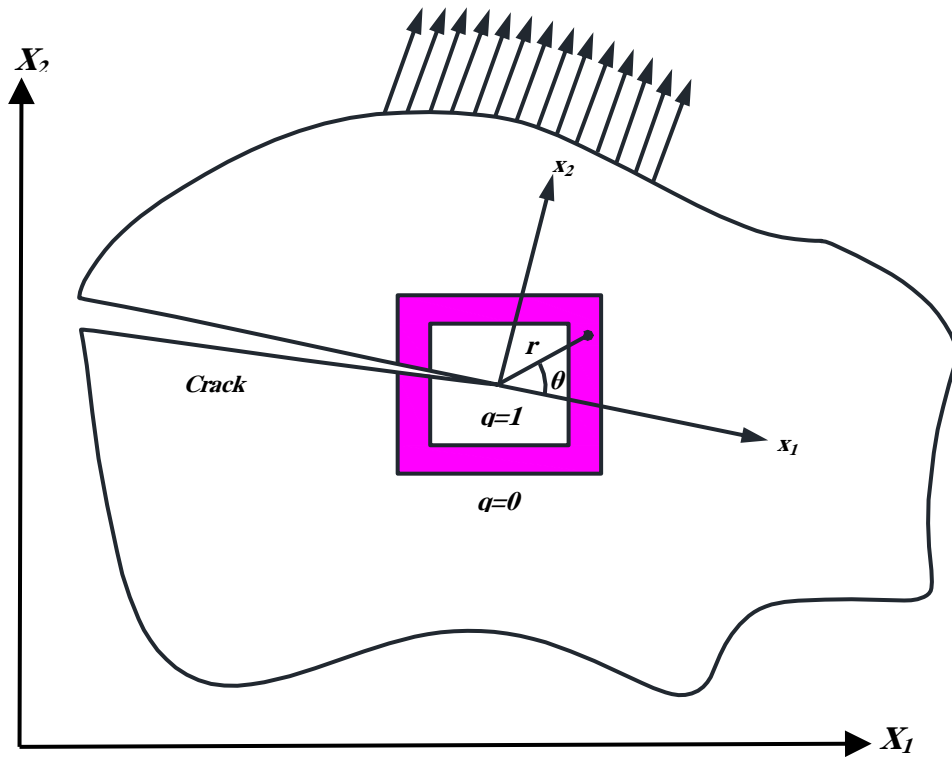
Figure (2): Equivalent domain integral
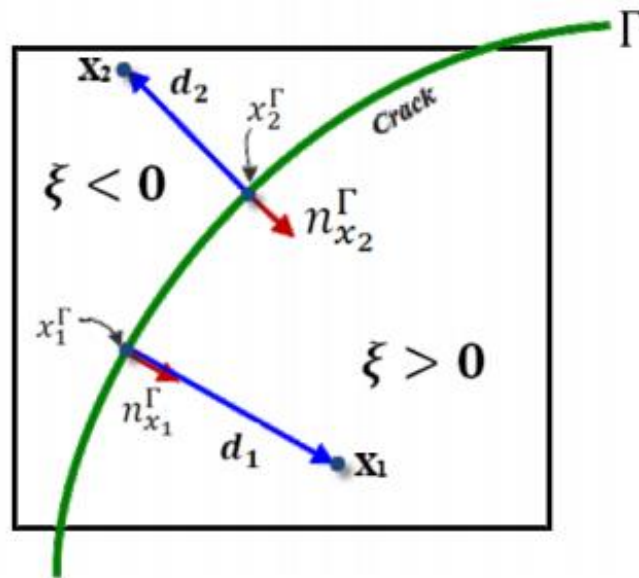
Figure (3): Sign distance function parameters [19]
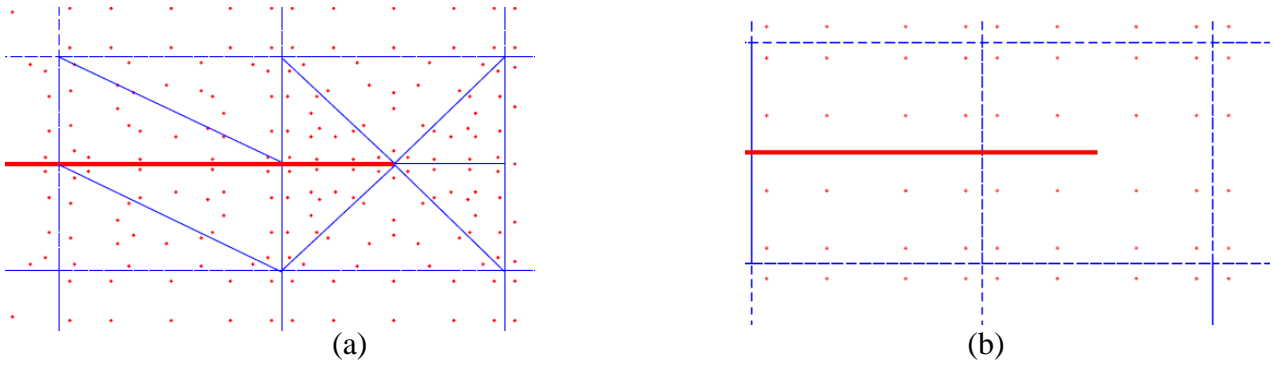
Figure (4): Gauss points around the crack: (a) sub-triangles technique and (b) conventional (ordinary) distribution [21]
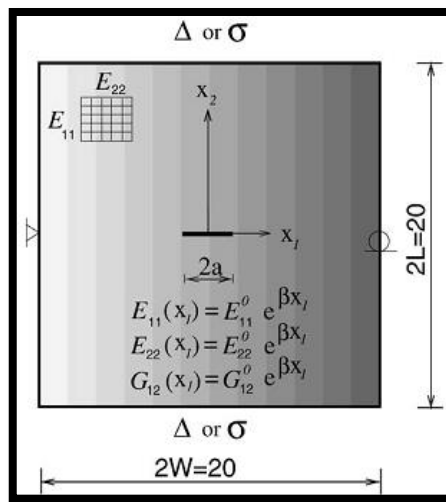
Figure (5): Complex FG plate with a crack parallel to material gradation.
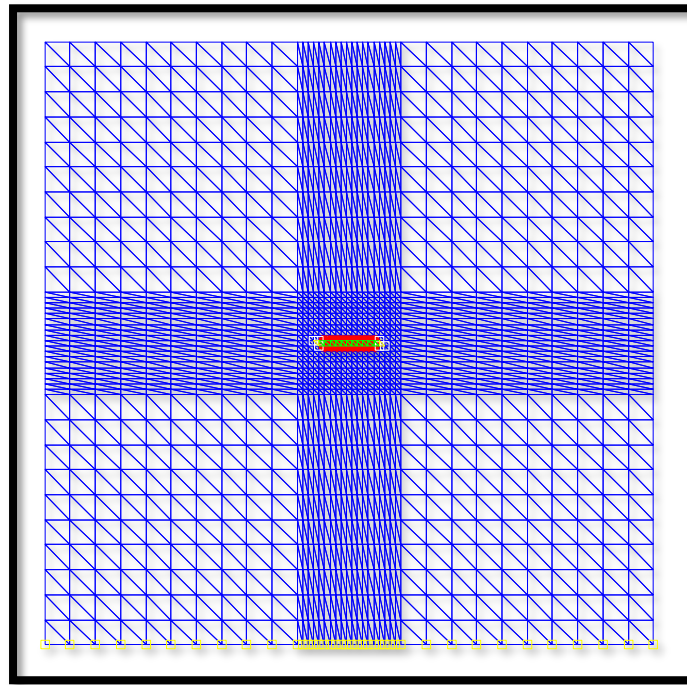
Figure (6): structured mesh of whole domain; the crack is modeled by level set method
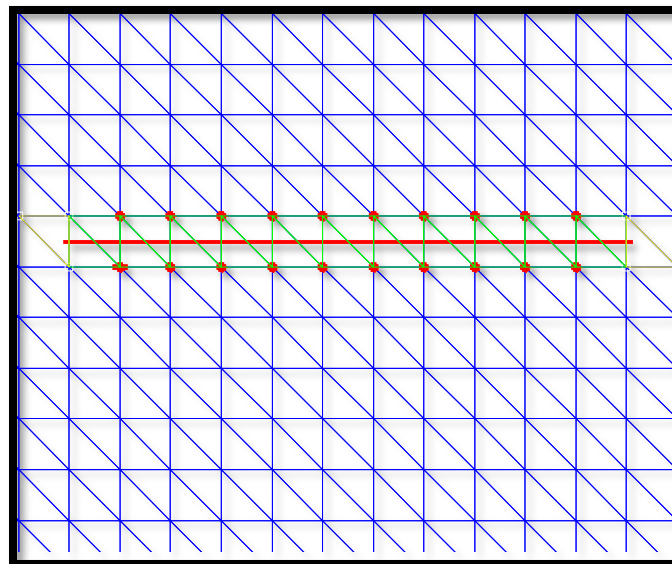
Figure (7): zoom for crack region
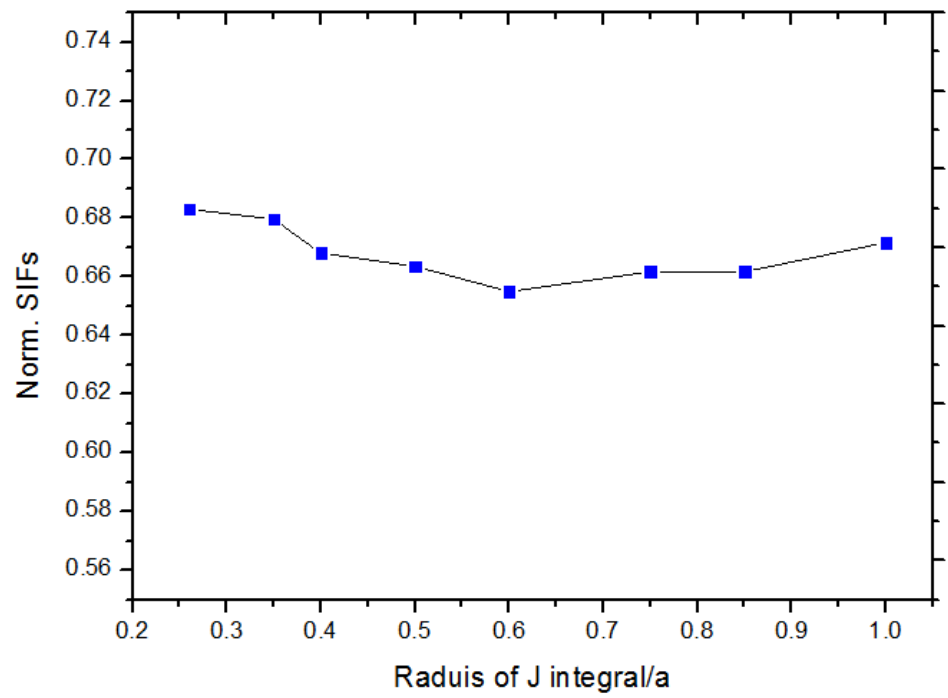
Figure (8): the verification of the present work that occurred between the radius of J integral and normalized SIF